

Research Article

Characterization of Mechanical Properties: Low-Density Polyethylene Nanocomposite Using Nanoalumina Particle as Filler

Ching Yern Chee,¹ N. L. Song,² Luqman Chuah Abdullah,^{2,3} Thomas S. Y. Choong,² Azowa Ibrahim,⁴ and T. R. Chantara⁵

¹ Department of Mechanical Engineering, Faculty of Engineering, University of Malaya, 50603 Kuala Lumpur, Malaysia

² Department of Chemical and Environmental Engineering, Faculty of Engineering, Universiti Putra Malaysia, Selangor, 43400 Serdang, Malaysia

³ Institute of Tropical Forestry and Forest Product, Universiti Putra Malaysia, Selangor, 43400 Serdang, Malaysia

⁴ Department of Chemistry, Faculty of Science, Universiti Putra Malaysia, Selangor, 43400 Serdang, Malaysia

⁵ Radiation Processing Technology Division, Malaysian Nuclear Agency, Bangi, 43000 Kajang, Malaysia

Correspondence should be addressed to Ching Yern Chee, chingyc@um.edu.my

Received 2 July 2012; Revised 21 September 2012; Accepted 6 October 2012

Academic Editor: Fathallah Karimzadeh

Copyright © 2012 Ching Yern Chee et al. This is an open access article distributed under the Creative Commons Attribution License, which permits unrestricted use, distribution, and reproduction in any medium, provided the original work is properly cited.

Nanocomposites based on low-density polyethylene (LDPE), containing 0.5, 1, 2, 3, and 5 wt% of nanoalumina, were prepared by melt-mixing at 125°C and hot melt-pressing to thin polymer film at 125°C. To enhance the interfacial interaction between alumina and LDPE, alumina surface was treated with silane which acts as coupling agent. The effects of alumina additions to the structure and morphology of LDPE matrix were characterized using Fourier transform infrared spectroscopy (FTIR) and scanning electron microscopy (SEM), respectively. The mechanical behaviour of nanoalumina-reinforced LDPE composite was studied using tensile tests, flexural tests, and impact tests. The interfacial adhesion between nano alumina particle and LDPE matrix was investigated. The result showed that the reinforcement performance of nano alumina to LDPE matrix was attributed to the interfacial adhesion between nanoparticle and polymer matrix. The addition of 1 wt% nano alumina has successfully enhanced the mechanical properties of LDPE material.

1. Introduction

There are always critical needs for lighter, stronger, less expensive, and more versatile materials to meet the demands of industrial consumers. The synthesis of polymer nanocomposite is an integral aspect of polymer nanotechnology. Polymer nanocomposite has been known as one of the early success stories of realizing the potential of nanomaterial as reinforcement filler to improve the properties of neat polymers. By adding the nanosized organic compounds, the properties of polymers are improved [1, 2]. Properties of the nanocomposites produced are depending on the inorganic materials present in the polymers matrix [1–6].

Generally, the efficiency of reinforcing fillers in the matrix is inversely proportional to the size of fillers and proportional to the ratio blend in the matrix. Therefore, the geometry of the filler is an important factor which affects the reinforcement performance of the nanoparticles-filled composites. When the surface to volume ratio of the filler is greater, the blending result will become more effective [4, 7]. The reason for this useful behaviour is that when characteristics structural features are intermediate in extent between isolated atoms and bulk macroscopic materials, the objects may display physical attributes substantially different from those displayed by either atoms or bulk materials [8, 9].

Polymers can be mixed with different kinds of clay materials [10, 11]; however, there is still lack of works has

been reported on others types of ceramics such as alumina. Alumina is well known for its mechanical properties such as extremely strong and achieves the highest stiffness among the oxide ceramics. Besides, the excellent dielectric properties, refractoriness, high hardness, and good thermal properties of alumina have contributed to its high usage in wide range of applications. The smaller particle size of ceramic has further enhanced its mechanical strength and so for alumina.

Nanoparticles normally exist in two forms during dry state. Strong bonds due to sintering will hold the primary particles to exist in aggregated form. The particles will exist in agglomerated form with weak bonding of van der Waals forces. Several methodologies have been used to overcome and separate the weaker attractive forces between the agglomerated nanoparticle samples [12]. However, the nanoparticles in aggregated forms cannot be separated. Uniform dispersion of fillers within polymer matrix will further enhance the reinforcement effectiveness of the fillers to the properties of polymer matrix. At this moment, ultrasonication is one of the common methods to disperse fillers before compounding process during nanocomposite fabrication. In this study, Fourier transform infrared spectroscopy (FTIR) study was performed to identify the chemical composition of nanocomposite. The mechanical properties of nanocomposites such as tensile, flexural, and impact were evaluated and discussed. The morphology and failure formation were investigated using scanning electron microscope (SEM). The aims of this study were to investigate the effect of nanoalumina particles to tensile, flexural, and impact properties of LDPE material.

2. Experimental

2.1. Materials. The polyethylene matrix used in this study was low-density polyethylene (LDPE) copolymer resin grade TITANLENE LDI 305YY supplied by Titan Group Sdn. Bhd. The density of the polymer was specified as 0.923 g/cm^3 . The ceramic filler used was alumina produced using sol-gel method with particle size ranges between 10 to 40 nm. To achieve uniform dispersion of filler, an anionic surfactant, sodium dodecylbenzenesulfonate (SDBS) from MERCK was added during the blending process.

2.2. Alumina Nanoparticle Preparation. Alumina nanoparticles were synthesized by using sol-gel method which have particle sizes between 10 to 40 nm. Aluminum isopropoxide $\text{Al}(\text{OC}_3\text{H}_7)_3$ (Merck, German), aluminum nitrate $\text{Al}(\text{NO}_3)_3 \cdot 9\text{H}_2\text{O}$ (Merck, German), sodiumbis-2-ethylhexyl sulfosuccinate ($\text{Na}(\text{AOT})$) (Merck, German), and 1/3-benzene disulfonic acid disodium salt (SDBS) (Merck, German) were used as raw materials to prepare nano- $\alpha\text{-Al}_2\text{O}_3$. The starting solution was prepared through using aluminum isopropoxide and 0.5 M aluminum nitrate aqueous solution as a solvent. The molar ratio of alumina sol (ALP/ALN) was 3 : 1. The solutions were continuously stirred for 48 hrs. Then, the sodium bis-2-ethylhexyl sulfosuccinate ($\text{Na}(\text{AOT})$) and 1/3-benzene disulfonic acid disodium salt (SDBS) were added by adjusting the molar ratio between

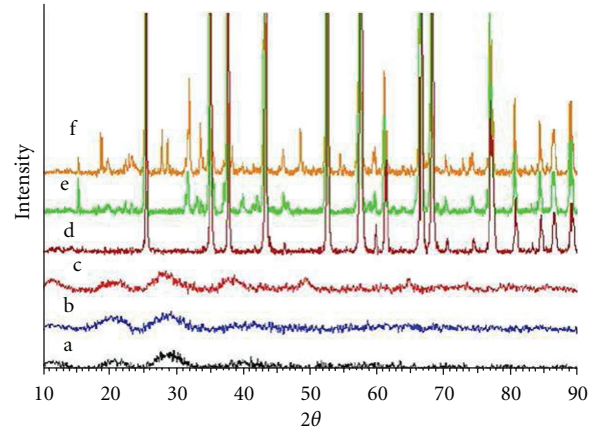


FIGURE 1: XRD spectra of aluminum oxide obtained under various conditions: (a) XRD spectrum of boehmite formed without surface stabilizer before calcined, (b) XRD spectrum of boehmite formed after the addition of $\text{Na}(\text{AOT})$ before calcined, (c) XRD spectrum of boehmite formed after the addition of SDBS before being calcined, (d) XRD spectrum of $\alpha\text{-Al}_2\text{O}_3$ formed without surface stabilizer, after calcined at 1200°C , (e) XRD spectrum of $\alpha\text{-Al}_2\text{O}_3$ formed after the addition of $\text{Na}(\text{AOT})$ after calcined at 1200°C , and (f) XRD spectrum of $\alpha\text{-Al}_2\text{O}_3$ after the addition of SDBS after calcined at 1200°C .

alkoxide and surfactants to be 0.1 and stirred for 1 hr. It is expected that this time is the optimal time for the addition of surfactant and it occurs prior to the onset of the nucleation and growth step. The solutions were heated up to 60°C and stirred constantly for evaporation process. Viscosity and color changed as the sol turned into a transparent stick gel. The gels were then heat treated at 90°C for 8 hr. Dried gels were calcined at temperature 1200°C . Finally, the calcined powders crushed by using mortar and pestle.

Phase identifications were performed by X-ray diffraction (XRD) using nickel filtered $\text{CuK}\alpha$ radiation in the range of $2\theta = 10\text{--}80^\circ$ with a scanning speed of 58/min. The XRD analysis in Figure 1 showed the most stable phase, $\alpha\text{-Al}_2\text{O}_3$ occurred dominantly at 1200°C . The observation indicated that completion of the most stable phase, α -alumina occurs at this temperature. Although the thermodynamically stable $\alpha\text{-Al}_2\text{O}_3$ phase can be obtained through a sequence of topotactic and reconstructive transformations (i.e., boehmite $\rightarrow \gamma \rightarrow \delta \rightarrow \theta \rightarrow \alpha$), the morphology remains unchanged and the final products have the same shape as the initial phases. Alumina was dispersed using ultrasonic bath (Branson 1510) for 1 hr at room temperature with the present of surfactant used for dispersion of alumina and surface treatment. Transmission electron microscopy (TEM) was performed to ensure the alumina produced were in nanosized and well dispersed (Figure 2).

2.3. Composites Preparation. Nanoalumina was first dispersed using Branson 1510 ultrasonic bath for 1 h before compounding process. The nanoalumina particles were then compounded with LDPE matrix using Haake PolyDrive at operating temperature of 125°C and speed at 80 rpm min^{-1} for 12 min.

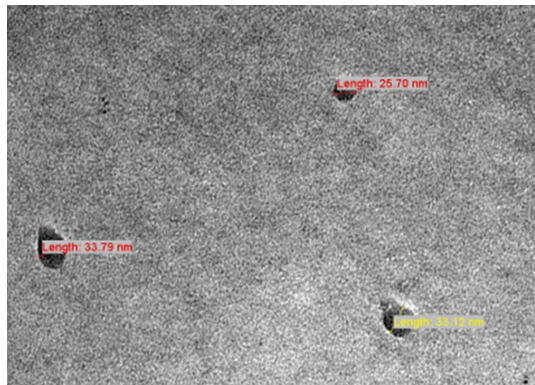


FIGURE 2: TEM image of dispersed nanoalumina particle.

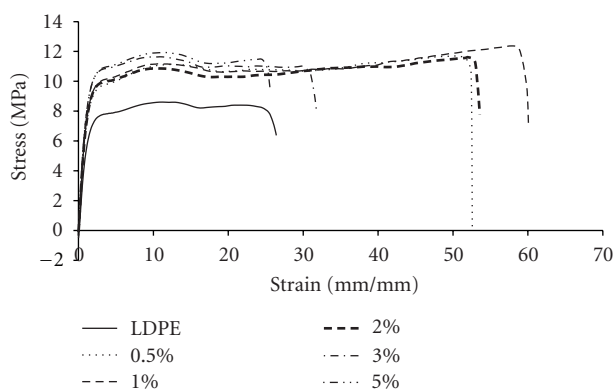


FIGURE 3: Typical stress-strain curves of neat LDPE and LDPE/alumina nanocomposites.

2.4. Characterization. Fourier transform infrared spectroscopy (FTIR) studies were carried out to determine the functional groups and types of bonding of the samples. FTIR spectra were measured using Perkin Elmer Spectrum 1000 FTIR spectrometer equipped with ATR. The infrared spectra were recorded between frequency ranges from 400 to 4000 cm^{-1} .

For mechanical properties studies, the test specimens for tensile, flexural, and impact tests were moulded and cut according to dimension specified in ASTM D638-03, ASTM D790-03, and ASTM D256-06a, respectively. Both of the tensile and flexural tests were measured using INSTRON Machine Model 4302 under atmospheric conditions. Average 5 samples were tested and the stress-strain curves were recorded. Crosshead speed for tensile and flexural tests was carried at 5 mm/min and 1 mm/min, respectively. The notched Izod impact test was carried out using Impact Pendulum Tester (Model Ceast CE UM-636) equipped with 4 J hammer. The morphologies of failure surfaces from tensile tests were investigated using Scanning Electron Microscope S-3400N (Hitachi).

3. Results and Discussion

The IR spectra of nanocomposites sample were studied between the absorption ranges of 400–4000 cm^{-1} . The characteristic absorption peaks for stretch and bend vibrations

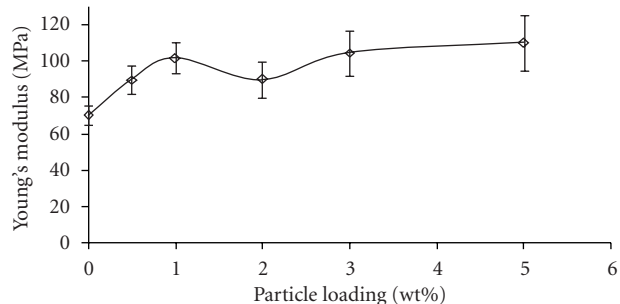


FIGURE 4: Effect of nanoalumina particles to Young's modulus properties of LDPE.

LDPE were 2912.55, 2849.05, 1464.16, and 719.45 cm^{-1} , respectively. The IR spectrum showed that there was no any chemical reaction and new bonding formed from the blending of LDPE and nanoalumina particles.

Stress-strain curves from tensile tests for LDPE/alumina nanocomposites are shown in Figure 3. Figure 3 shows that the stress at break gradually increased with the increasing of alumina loading up to 1 wt%. This result suggests that the fine alumina particle would reinforce and orient along the direction of stress, and this has contributed to the increase of tensile strength of the nanocomposite with the addition of 0.5 and 1 wt% of alumina particles.

The stress-strain curves also illustrates that there was a significant increase of elongation at break values of LDPE with the incorporation of alumina particle into the nanocomposite. This result indicates that the incorporation of alumina particle would improve the interaction between the molecules. At lower weight percentage, the addition of alumina in LDPE matrix increases surface interaction bonding between the molecules. The nanoparticles may be trapped inside entanglements and resulted in a restriction on the polymer overall chain mobility both near and far-field to the filler surface.

Figure 3 shows that both of the stress at break and elongation at break (strain) of nanocomposite achieved the highest values with 1 wt% loading of alumina particles. Above 1 wt% alumina loading, both the stress and elongation at break showed a gradual drop. These results are attributed to the reinforcing effect of the alumina particles. The higher amount of alumina particles would reduce the reinforcing effect and mechanical properties of the nanocomposite due to poor dispersion and agglomeration of alumina particles. The agglomerated alumina particles with larger particle size would serve as flaws and stress concentration for crack initiation, resulting in poor tensile properties [14, 15]. In this study, the nanoparticles were well dispersed at lower loading (0.5 to 1 wt%) of alumina particles. The reinforcing effect of this small amount of nanoparticle loadings with huge specific surface area has dramatically larger total interface area for reinforcement efficiency [9].

Figure 4 illustrates the effect of nanoalumina particles to Young's modulus of LDPE matrix. As shown in the Figure 4, Young's modulus increased with the addition of alumina nanoparticles. This suggests that the incorporation

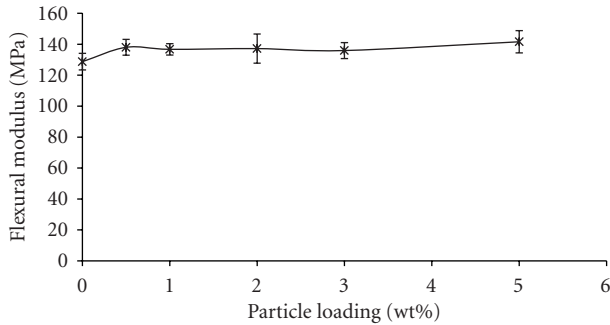


FIGURE 5: Effect of nanoalumina particle loadings to flexural modulus of LDPE matrix.

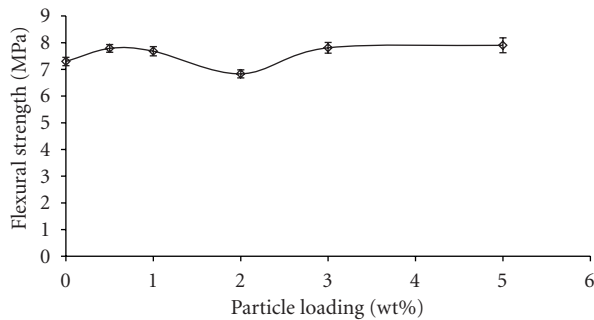


FIGURE 6: Effect of nanoalumina particle loadings to flexural modulus of LDPE matrix.

of alumina nanoparticles would improve the stiffness of LDPE. However, the further increment of particle loadings did not give significant improvement to Young's modulus. With the higher particle loadings, agglomerations take place and reduce the total surface area of the nanoparticles.

At low alumina contents of 1 wt%, the nanocomposite exhibits an interactive structure with matrix. Strong interfacial interaction will enable the load to be transferred easily across the nanoparticles-matrix interface. This will contribute to the increase of Young's modulus and tensile strength of the nanoparticles reinforced composite. These improvements in mechanical properties also proved that the interaction between the polymer matrix and nanoparticles has successfully restricted the yielding of massive matrix [9]. However, the agglomeration of particles happened with the increasing of alumina loadings. The high amount of nanoparticle loadings did not participate in homogeneous interactive bonding with LDPE. The weak interaction between particle and matrix has caused lower tensile properties due to the debonding of particle from matrix prior to the plastic deformation of the matrix [9].

Figure 5 shows the effect of alumina loading on flexural properties of LDPE. The introduction of alumina particles to the specimen did not show significant effect to the flexural modulus of LDPE (Figure 5). However, flexural strength of the nanocomposite reduced with the addition of nanoalumina particles >1 wt% as shown in Figure 6. There are few factors that affect the flexural properties of filler reinforced polymer which includes the degree of

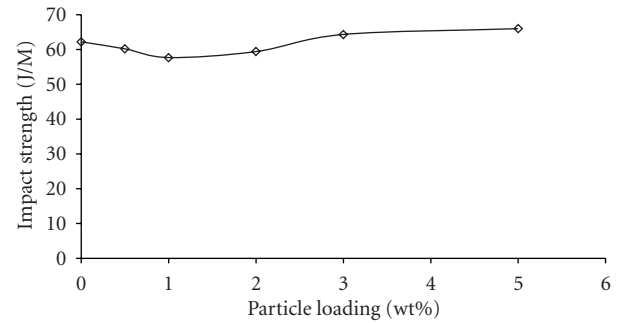


FIGURE 7: Effect of nanoalumina particle loadings to impact strength of LDPE.

dispersion filler, aspect ratio of the filler, and adhesion at the filler-matrix interface [16, 17]. The treatment layer has been introduced on the alumina particles surface so that it become hydrophobic which same as LDPE [16]. However, the polarity of alumina particles and LDPE is different. Thus, the weak interfacial regions in LDPE/nanoalumina composite are attributed to the incompatible between polar alumina particles filler and nonpolar LDPE.

The notched impact strength of LDPE/alumina nanocomposites with various particle loadings is shown in Figure 7. It is apparent from Figure 7 that the impact strength shows a downward trend till 1 wt% alumina loading. The impact strength was then gradual increase when the loading of alumina particles was >1 wt%.

The decrease of impact strength at low wt% alumina addition might be caused by the poor interfacial adhesion between the matrix and nanoparticles. The weak interfacial adhesion would cause an increase or a greater extent of cavitation or voiding [16, 18]. The particles in the matrix had initiated the crack in the LDPE and caused the failure. With the increasing of the alumina particles, the specimens became more brittle and more particles would function as terminator of craze. This would bring advantage to the percolation of the yielding process over the LDPE matrix, thus contribute to greater improvement to the Izod impact strength of the nanocomposites [19]. The toughening mechanisms are thought to be associated with debonding of particles. This prevents crazing of the polymer matrix and allows extensive plastic deformation, resulting in high fracture toughness.

A regular dispersion of the nanoparticles in the matrix is absolutely necessary for obtaining the reinforcing effect in the case that nanoparticles are used. This is depending on the microstructure of composites, in addition to the interfacial bonding as well as shape and dimension of the filler, its spatial distribution in the matrix, the width of the interface. While the broke bonding is between the matrix and the filler, the composite is weak for the reason that the functional load cannot be transferred to the filler. The decreasing of tensile strength was supported by Gojny et al. [20], whereby it was supposed that the minor decline in tensile strength value at higher nanofiller content can be certified to the rising amount of unacceptable impregnated agglomerates, which

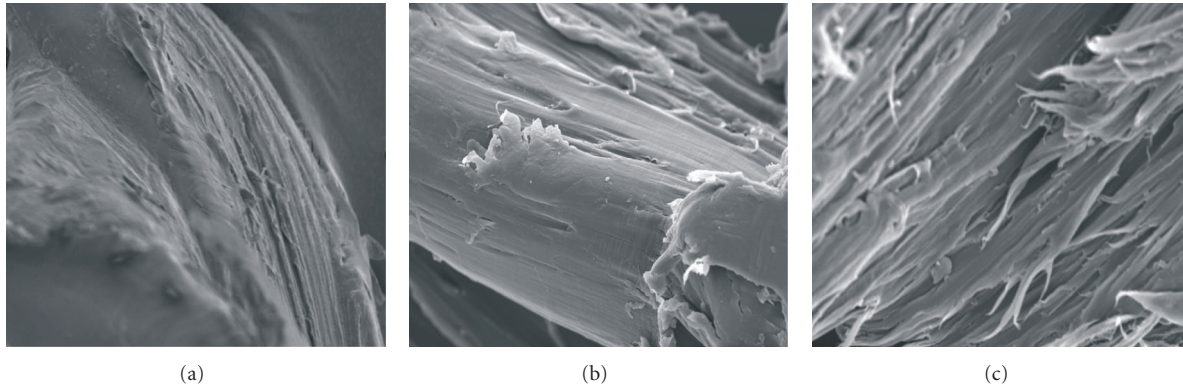


FIGURE 8: SEM micrographs for tensile fracture surface of LDPE/alumina composite containing (a) 0 wt%, (b) 1.0 wt%, and (c) 5.0 wt% of nanoalumina particles. (Mag. 550 x).

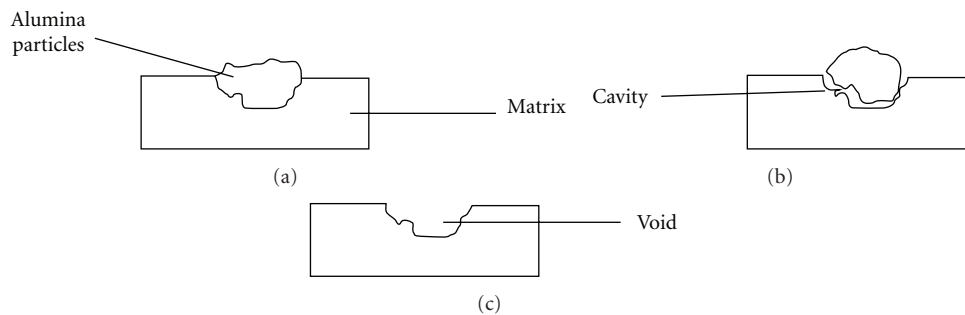


FIGURE 9: Schematic representation of particle-matrix debonding in polymer matrix composites (Rashid et al. [13]).

performing imperfections in the composites, reminding untimely failure. Li [21] presented the creation of filler agglomeration site inside the matrix body that possibly acts as et al. the failure initiation sites which might help the propagation of the crack or fracture. This problem becomes more critical, when the content of nano α - Al_2O_3 is too high.

SEM micrographs of LDPE/alumina nanocomposites at 0, 1, and 5 wt% of alumina loading are shown in Figure 8. Figure 8(a) shows a smooth surface for pure LDPE. There was formation of small amount of fibril after tensile test on fracture surface of LDPE/nanoalumina composite reinforced with 1 wt% of nanoalumina particles. (Figure 8(b)). Previous researches [22, 23] had reported that the yield points often induced in the stress-strain curves of the ductile polymers reinforced with the rigid fillers. This yielding phenomenon is normally caused by the effect of crazing or dewetting where the adhesion between the filler and matrix phases was destroyed [23]. So, it was believed that the formation of fibril in LDPE/alumina composite was caused by the effect of crazing or dewetting.

Figure 8(c) shows that the number of fibril formations on fracture surface of composite increased with the increasing of alumina loadings. This illustrates that the adhesion between nanoparticle and matrix decreases with the increasing of nanoalumina loadings. Due to the absence of particle-matrix interaction, the particles tend to agglomerate and become unevenly distributed throughout the matrix. As

the consequence, the nanocomposite showed tendency for shear yielding when the loads were applied on it. These observations support the tensile results where nanocomposite with 1 wt% of alumina particles displayed higher tensile strength compared to sample containing 5 wt% of nanoalumina particles.

Tohgo and Itoh [24] reported that if the debonding of the particles occurs, there would be a broad plastic deformation. Once the adhesion is lower down, debonding can happen and consequently crazing is concealed and the yield mechanisms develop into operative. Plastic deformation of the matrix polymer is the major energy absorbing process and this rising interaction between particles and polymer is lowered. The holes where the alumina particles were removed from the LDPE matrix during elongation demonstrate very poor bonding between them. The elongated interfaces illustrate the occurrence of plastic deformation. This finding agreed with the results of Rashid et al. [13].

They presented numerous statements to explain the procedure of shear yielding and debonding. At first, the debonding is mostly controlled by the stress of the particles and the statistical behavior of the particle-matrix interfacial strength (Figure 9(a)). For the duration of debonding (Figure 9(b)), the stress of the deboned particles is unrestricted and the position of the particle is regarded like a void. A volume fraction of the deboned particles turns into a void (Figure 9(c)). At 5 wt% nano α -alumina content, extensive

surface coarseness is obviously seen which crack improved. Impeded plastic deformation decreases tensile and flexural properties and failure strain. Interfacial adhesion becomes much weaker at higher α -alumina concentration owing to pitiable particle wetting by the matrix as compared to lower α -alumina content. This occurrence will permit crack to broadcast at quicker rate (less adhesion) which effects in the morphological suggestion.

4. Conclusions

LDPE material reinforced with varying composition of nano-alumina particles treated with silanes has been prepared for mechanical and morphology studies. The IR spectrum from FTIR analysis indicated that there was no chemical reaction between LDPE matrix and alumina particles. The effect of incorporation of 0.5–5 wt% of alumina particles to tensile, flexural, and impact properties of LDPE matrix were investigated. The results showed that the addition of 1 wt% of nanoalumina has successfully enhanced the tensile and elongation at break of the nanoalumina filled LDPE material. The incorporation of >1 wt% of nanoalumina particles had caused agglomeration and uneven distribution of the particles throughout the LDPE matrix.

Acknowledgments

This work was supported by University Malaya Research (Grant: UMRG RG125-11AET), and NSFC under Grant no. 60973089.

References

- [1] Y. C. Ching and I. I. Yaacob, "Effect of polyurethane/nanosilica composites coating on thermo-mechanical properties of polyethylene film," *Materials Technology*, vol. 27, no. 1, pp. 113–115, 2012.
- [2] Y. C. Ching, C. Y. Chen, and I. I. Yaacob, "Weathering resistance of solventborne polyurethane/nanosilica composite," *Advanced Science Letters*, vol. 12, no. 1, pp. 165–169, 2012.
- [3] A. Lagashetty and A. Venkataraman, "Polymer nanocomposites," *Resonance*, pp. 49–60, 2005.
- [4] C. Y. Chee and I. I. Yaacob, "Influence of nanosilica/polyurethane composite coating on IR effectiveness and visible light transmission properties of polyethylene," *Advanced Materials Research*, vol. 97–101, pp. 1669–1672, 2010.
- [5] S. Li, S. Zhang, S. Zhou, G. Gu, and L. Wu, "Physical and optical properties of silica/polymer nanocomposite inverse opal," *Advanced Science Letters*, vol. 4, no. 11-12, pp. 3445–3450, 2011.
- [6] C. Y. Chee and I. I. Yaacob, "Influence of nano-sio2/polyamide composites coating on thermic effect and optical properties of polyethylene film," *International Journal of Modern Physics B*, vol. 23, no. 6-7, pp. 1395–1400, 2009.
- [7] C. J. Chou, A. E. Read, E. I. Garcia-Meitin, and C. P. Bosnyak, *Polymer Nanocomposite*, The Dow Chemical Company, Midland, Mich, USA, 2002.
- [8] Z. Wang, J. Ruan, and D. Cui, "Advances and prospect of nanotechnology in stem cells," *Nanoscale Research Letters*, vol. 4, no. 7, pp. 593–605, 2009.
- [9] H. X. Zhao and K. Y. Li, "Crystallization, mechanical, and fracture behaviors of spherical alumina-filled polypropylene nanocomposites," *Journal of Polymer Science B*, vol. 43, no. 24, pp. 3652–3664, 2005.
- [10] S. Hotta and D. R. Paul, "Nanocomposites formed from linear low density polyethylene and organoclays," *Polymer*, vol. 45, no. 22, pp. 7639–7654, 2004.
- [11] A. Durmus, A. Kaşgöz, and C. W. Macosko, "Mechanical properties of linear low-density polyethylene (LLDPE)/clay nanocomposites: estimation of aspect ratio and interfacial strength by composite models," *Journal of Macromolecular Science B*, vol. 47, no. 3, pp. 608–619, 2008.
- [12] N. Mandzy, E. Grulke, and T. Druffel, "Breakage of TiO₂ agglomerates in electrostatically stabilized aqueous dispersions," *Powder Technology*, vol. 160, no. 2, pp. 121–126, 2005.
- [13] E. S. A. Rashid, H. M. Akil, K. Ariffin, and C. K. Chee, "The flexural and morphological properties of α -alumina filled epoxy composites," *Malaysian Polymer Journal*, vol. 1, no. 1, pp. 25–38, 2006.
- [14] B. Yalcin and M. Cakmak, "The role of plasticizer on the exfoliation and dispersion and fracture behavior of clay particles in PVC matrix: a comprehensive morphological study," *Polymer*, vol. 45, no. 19, pp. 6623–6638, 2004.
- [15] C. Chen, A. Wang, and L. Fei, "Effects of ultrasonic on preparation of alumina powder by wet chemical method," *Advanced Science Letters*, vol. 4, no. 3, pp. 1249–1253, 2011.
- [16] R. C. Willemsse, A. Posthuma De Boer, J. Van Dam, and A. D. Gotsis, "Co-continuous morphologies in polymer blends: a new model," *Polymer*, vol. 39, no. 24, pp. 5879–5887, 1998.
- [17] C. Subramani, V. S. Jamnik, and S. T. Mhaske, "Effect of attapulgite filler on the properties of nylon-6," *Polymer Composites*, vol. 29, no. 8, pp. 890–893, 2008.
- [18] J. M. Willis, B. D. Favis, and J. Lunt, "Reactive processing of polystyrene-co-maleicanhydride/elastomer blends: processing-morphology-property relationships," *Polymer Engineering & Science*, vol. 30, no. 17, pp. 1073–1084, 1990.
- [19] H. Yang, Q. Zhang, M. Guo, C. Wang, R. Du, and Q. Fu, "Study on the phase structures and toughening mechanism in PP/EPDM/SiO₂ ternary composites," *Polymer*, vol. 47, no. 6, pp. 2106–2115, 2006.
- [20] F. H. Gojny, M. H. G. Wichmann, B. Fiedler, and K. Schulte, "Influence of different carbon nanotubes on the mechanical properties of epoxy matrix composites—a comparative study," *Composites Science and Technology*, vol. 65, no. 15-16, pp. 2300–2313, 2005.
- [21] G. Y. Li, P. M. Wang, and X. Zhao, "Mechanical behavior and microstructure of cement composites incorporating surface-treated multi-walled carbon nanotubes," *Carbon*, vol. 43, no. 6, pp. 1239–1245, 2005.
- [22] R. A. Zoppi, C. R. De Castro, I. V. P. Yoshida, and S. P. Nunes, "Hybrids of SiO₂ and poly(amide 6-b-ethylene oxide)," *Polymer*, vol. 38, no. 23, pp. 5705–5712, 1997.
- [23] L. E. Nielsen and R. F. Landel, *Mechanical Properties of Polymers and Composites*, vol. 90, CRC Press, New York, NY, USA, 1994.
- [24] K. Tohgo and T. Itoh, "Elastic and elastic-plastic singular fields around a crack-tip in particulate-reinforced composites with progressive debonding damage," *International Journal of Solids and Structures*, vol. 42, no. 26, pp. 6566–6585, 2005.



Hindawi

Submit your manuscripts at
<http://www.hindawi.com>

